Available online at www.sciencedirect.com

ScienceDirect

Energy Procedia 145 (2018) 32–37

Energy Procedia

www.elsevier.com/locate/procedia

Applied Energy Symposium and Forum, Renewable Energy Integration with Mini/Microgrids, REM 2017, 18–20 October 2017, Tianjin, China

Hierarchical Power Flow Control of a Grid-tied Photovoltaic Plant Using a Battery-Supercapacitor Energy Storage System

Mukalu Sandro Masaki*, Lijun Zhang, Xiaohua Xia

Department of Electrical, Electronic and Computer Engineering, University of Pretoria, Pretoria 0002, South Africa

Abstract

A two-layer power flow control for a grid-tied photovoltaic plant equipped with battery-supercapacitor energy storage system is presented in this paper. The proposed strategy aims at simultaneously handling the intermittent nature of the solar radiation received by the photovoltaic collectors and the need to consistently supply the specified power taking advantage of the complementary characteristics of the energy storage technologies. It relieves the batteries from stress through the use of the photovoltaic and the supercapacitor to supply the high frequency power demands by means of hierarchical control. Extensive simulation results confirm the effectiveness of the proposed power flow control strategy.

Keywords: Renewable energy; Power smoothing; Hybrid energy storage system; Optimal control; Photovoltaic; Supercapacitor.

1. Introduction

Large-scale integration of solar photovoltaics (PVs) into power systems is being implemented at a steady pace worldwide as a result of the ever-growing electricity demand and the environmental nuisance caused by the burning of fossil fuels. The resulting increase in the proportion of weather-dependent generation, however, brings in potential risks for the power quality of the existing power grid.

Among the popular solutions to improve the dispatchability of solar PV systems is the integration of hybrid energy storage systems (ESSs) [1]. Unlike single storage technologies, the hybrid ESS, comprising two or more

* Corresponding author. Tel.: +27-(0)12-420-2068.
E-mail address: sandro.masaki@up.ac.za.

10.1016/j.egypro.2018.04.007

different storage technologies, can economically achieve at the same time the two main functions required for power supply: fast response and long-term energy support [2]. Due to maturity and feasibility reasons, the battery-supercapacitor (SC) combination is currently the most preferred hybrid ESSs [3]. The batteries have high energy density but slow power response, while SCs are characterized by high power density and low energy capacity.

Some of the challenges inherent in such a hybrid ESS include achieving an effective power flow management between the various power system components, taking into account their individual specifications. In this regard, rule-based control strategies such as neural networks [2], floating average control [3] and heuristic control [4] are reported in the current literature. In general, their inability to handle weather forecast information affects their long-term performance negatively. On the other hand, the control strategies built on mathematical optimization focus either on the performance of hybrid ESSs [5] or the deviation between the output power of the plant and the set reference [6]. While the former ignores the interaction between the PV system and the main grid, the possibility to take advantage of forecasting techniques was not fully considered in the latter.

The remaining sections of this paper present a contribution intended to address the weakness identified above.

2. Problem formulation

The layout of a grid-tied solar PV-batteries-SCs system is shown in Fig. 1(a). The net power input of the solar PV onto the AC bus is represented by P_1, while P_2 and P_3 denote, respectively, the discharge and charge powers of the batteries. On the other hand, P_4 and P_5 denote the discharge and charge powers of the SCs, respectively. The power supplied to the main grid is represented by P_{out}. In order to control the power flow within the power system and that to the main grid, the power management unit (PMU) requires a periodic supply of information on the future solar radiation and the reference power P_{ref} issued.

The control approach proposed in this paper consists of two layers: an upper layer, indicated by the superscript L, and a bottom layer, indicated by the superscript S.

2.1. Upper layer power flow control

At the beginning of the dispatch period, the prediction of the solar radiation allows the estimate of the future solar PV generation $P_{pv}^L(k)$ at each sampling instant k ($k=1,\cdots,N_L$) of next N_L sampling instants of the upper layer control. Subsequently, considering the forecasted solar PV generation, the specifications of the solar PV power system and the expected demand, the grid operator assigns a fixed power profile P_{ref} to the system for the upcoming dispatch period.

The power flow control at the upper layer aims to reduce the deviation between P_{out} and P_{ref}, and maximize the use of solar energy available. The deviation between P_{out} and P_{ref} should also be maintained within a specific range as per the local power grid policies. To allow the control of the SC in the second layer, the energy range used by the first layer control is narrowed as shown in Fig. 1(b).

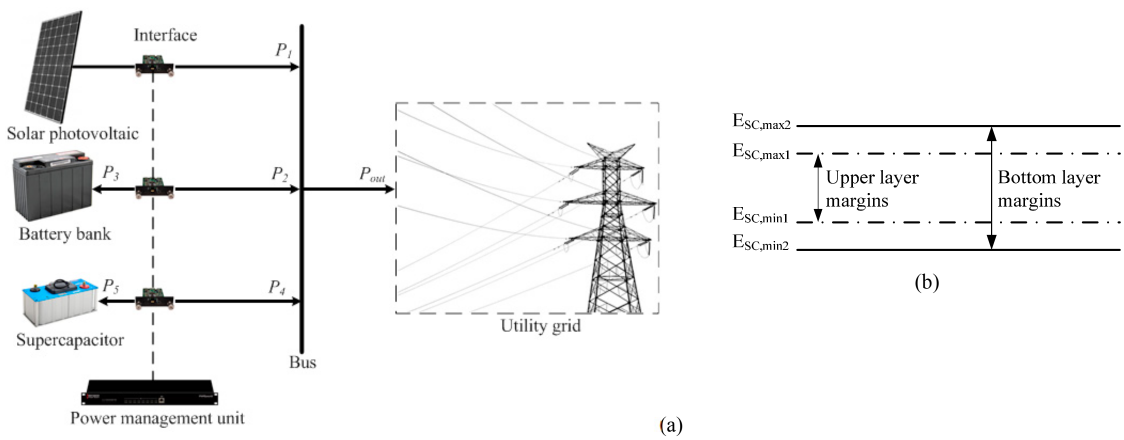

Fig.1. (a) Power system topology (b) SC energy margins at the upper and bottom layers.

The following optimization problem will be solved at the beginning of each dispatch period:

$$\min\ \alpha\sum_{k=1}^{N_L}\left(P_{out}^L(k)-P_{ref}(k)\right)^2+\left(1-\alpha\right)\sum_{k=1}^{N_L}\left(P_1^L(k)-P_{PV}^L(k)\right)^2, \tag{1}$$

subject to

$$P_2^L(k)P_3^L(k)=0, \tag{2}$$
$$P_4^L(k)P_5^L(k)=0, \tag{3}$$
$$\left(1-\varepsilon\right)P_{ref}(k)\le P_{out}^L(k)\le\left(1+\varepsilon\right)P_{ref}(k), \tag{4}$$
$$E_{B,\min}\le E_B^L(k)\le E_{B,\max}, \tag{5}$$
$$E_{SC,\min}+\left(1-\sigma\right)E_{SC,\max}\le E_{SC}^L(k)\le\sigma E_{SC,\max}, \tag{6}$$
$$0\le P_1^L(k)\le P_{pv}^L(k), \tag{7}$$
$$0\le P_2^L(k)\le P_{B,\max}, \tag{8}$$
$$0\le P_3^L(k)\le P_{B,\max}, \tag{9}$$
$$0\le P_4^L(k)\le P_{SC,\max}, \tag{10}$$
$$0\le P_5^L(k)\le P_{SC,\max}, \tag{11}$$

for all $k=1,\cdots,N_L$, where α is a weight factor ranging between 0 and 1, and $P_1^L(k)$, $P_2^L(k)$, $P_3^L(k)$, $P_4^L(k)$ and $P_5^L(k)$, are the control variables. The output power $P_{out}^L(k)$ is given by:

$$P_{out}^L(k)=P_1^L(k)+P_2^L(k)-P_3^L(k)+P_4^L(k)-P_5^L(k), \tag{12}$$

The energy content of the battery, denoted by $E_B^L(k)$ in (5), is expressed as follows:

$$E_B^L(k)=E_B(0)+\Delta T_L\eta_{B,c}\sum_{j=1}^{k}P_3^L(j)-\Delta T_L\eta_{B,d}\sum_{j=1}^{k}P_2^L(j), \tag{13}$$

where ΔT_L denotes the sampling period applied at the upper layer, $\eta_{B,c}$ denotes the battery charging efficiency, and $\eta_{B,d}$ denotes the battery discharging efficiency.

In (6), $E_{SC}^L(k)$ denotes the SC energy content and is obtained by:

$$E_{SC}^L(k)=E_{SC}^L(0)+\Delta T_L\eta_{SC,c}\sum_{j=1}^{k}P_5^L(j)-\Delta T_L\eta_{SC,d}\sum_{j=1}^{k}P_4^L(j), \tag{14}$$

for all $k=1,\cdots,N_L$, where $E_{SC}^L(0)$ denotes the initial SC energy content at the beginning of the current dispatch period, $\eta_{SC,c}$ and $\eta_{SC,d}$ denote the charging and the discharging efficiencies of the SC, respectively. In (6), the narrowing factor σ varies between $(E_{SC,min}+E_{SC,max})/(2E_{SC,max})$ and 1.

2.2. Bottom layer power flow control

Each sample interval k of the upper layer control is divided into even subintervals in the lower control layer. Shortly ahead of each subinterval, the PMU is supplied with updated solar radiation forecasts that are used to estimate an updated PV generation $P_{pv}^{S}(k,l)$ for each instant l ($l=1,\cdots,N_S$) of the N_S sampling instants of the coming interval k.

The bottom layer power flow control performed over every upper layer control interval aims at achieving objectives similar to the upper layer control, with however a few specificities. In particular, in case the dispatch cycle is maintained short enough and the corresponding forecasts in the upper layer are of an acceptable standard, the actual average solar PV generation at a sampling interval k of the dispatch period may be expected to remain in the vicinity of $P_{pv}^{L}(k)$. On the other hand, the relatively short sampling period applied in this layer may result in fast variation in the profile of P_{pv}^{S}, which should preferably not be handled by the batteries [3]. In view of the above, the batteries will not be involved in the bottom layer control, and their power setpoints received from the upper layer will be maintained. Next, the energy margins of the SCs will be set back to their rated values as shown in Fig. 1(b). Finally, to further improve the power quality, no overshooting of P_{ref} will be allowed at this stage.

The following optimization problem will be solved ahead of every sampling interval k of a dispatch period:

$$\min \beta \sum_{l=1}^{N_S} \left(P_{out}^{S}(k,l) - P_{ref}(k,l) \right)^2 + (1-\beta) \sum_{l=1}^{N_S} \left(P_1^{S}(k,l) - P_{PV}^{S}(k,l) \right)^2, \tag{15}$$

subject to

$$P_4^{S}(k,l) P_5^{S}(k,l) = 0, \tag{16}$$

$$(1-\varepsilon) P_{ref}(k,l) \le P_{out}^{S}(k,l) \le P_{ref}(k,l), \tag{17}$$

$$E_{SC,\min} \le E_{SC}^{S}(k,l) \le E_{SC,\max}, \tag{18}$$

$$0 \le P_1^{S}(k,l) \le P_{pv}^{S}(k,l), \tag{19}$$

$$0 \le P_4^{S}(k,l) \le P_{SC,\max}, \tag{20}$$

$$0 \le P_5^{S}(k,l) \le P_{SC,\max}, \tag{21}$$

for all $l=1,\cdots,N_S$, where β is a weight factor ranging between 0 and 1 and $P_1^{S}(k,l)$, $P_4^{S}(k,l)$ and $P_5^{S}(k,l)$ are the control variables. The SC energy content $E_{SC}^{S}(k,l)$ is be obtained by:

$$E_{SC}^{L}(k,l) = E_{SC}^{S}(k,0) + \Delta T_S \eta_{SC,c} \sum_{j=1}^{l} P_5^{S}(k,j) - \Delta T_S \eta_{SC,d} \sum_{j=1}^{l} P_4^{S}(k,j), \tag{22}$$

for all $l=1,\cdots,N_S$, where $E_{SC}^{S}(k,0)$ denotes the initial supercapacitor energy content at the beginning of the current bottom layer control. The output power $P_{out}^{S}(k,l)$ at the sampling instant l is given by:

$$P_{out}^{S}(k,l) = P_1^{S}(k,l) + P_2^{L}(k,l) - P_3^{L}(k,l) + P_4^{S}(k,l) - P_5^{S}(k,l), \tag{23}$$

where $P_2^{L}(k,l)$ and $P_3^{L}(k,l)$ are as previously determined by the upper layer.

3. Case study

A 1-MW solar PV power system approximated to one hectare is investigated in this study [7]. The reference power that applies to a given dispatch period is set equal to the geometric average of the solar PV generation calculated for the dispatch interval.

The hybrid ESS consists of a 250-kW/2630-kWh bank of lead-acid batteries and a 13.1-MW/5.74-kWh set of SCs. The permitted minimum and maximum energy contents of the storage equipment are fixed at 50% and 100% respectively for the batteries and 25% and 100% respectively for the SCs. The maximum power deviation coefficient ε is equal to 0.02.

4. Simulation Results and Discussions

The proposed control strategy was tested on a PC Core(TM) i3, 3.40 GHz, with 4 GB of RAM, running Windows 7. Classified as nonlinear programmings (NLPs), the above optimization problems were solved in the MATLAB environment using the "fmincon" function. Fig. 2(a) shows the comparison between $P_{out}^{L}(k)$ and P_{ref} (3a) for $\alpha=0.5$ and $\beta=0.5$. It is observed that the output power consistently tracks the reference issued by the grid operator, with very few deviations which are however maintained within the specified boundary. The 24-hour evolution of the state of charge (SOC), given in Fig. 2(b) shows the reduced stress of the battery through the slow variation of its SOC in comparison with the supercapacitor.

The superimposition of the forecasted PV generation at the upper and bottom control layers shown in Fig. 3(a) indicates the fast variations introduced by the forecast process at the bottom layer. The improved tracking of the reference power by the power plant is shown in Fig. 3(b). The increased involvement of the SC to achieve this performance during the control at the bottom layer is shown in Fig. 3(c) and (d).

The lengths of forecast periods at the upper layer and bottom layer were set at 5 minutes and 10 seconds, respectively. With respective average computation times of 54.01 milliseconds and 38.44 milliseconds, and respective maximum computation times of 199.98 milliseconds and 130.99 milliseconds, the proposed power flow control strategy therefore shows good online capabilities.

4. Conclusion

An optimization-based power smoothing strategy for a grid-tied PV plant-battery-supercapacitor system was presented in this paper. The proposed approach achieves an effective management of both the uncertainties and fluctuations of the solar resource by a two layer control of the power flow within the PV power plant. The battery's lifespan is also extended by a decreased stress during the operation.

Acknowledgements

The authors gratefully acknowledge the support for this work provided by the National Hub for Energy Efficiency and Demand Side Management.

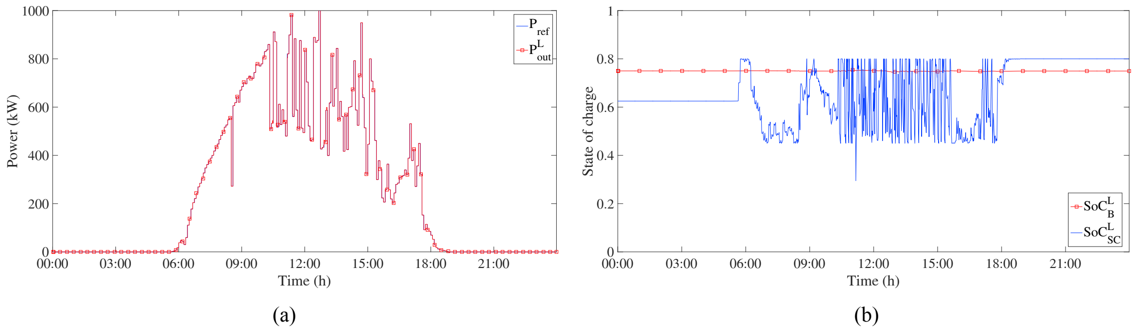

Fig.2. (a) Power reference tracking (α=0.5 and β=0.5) (b) Hybrid ESS state of charge (α=0.5 and β=0.5)

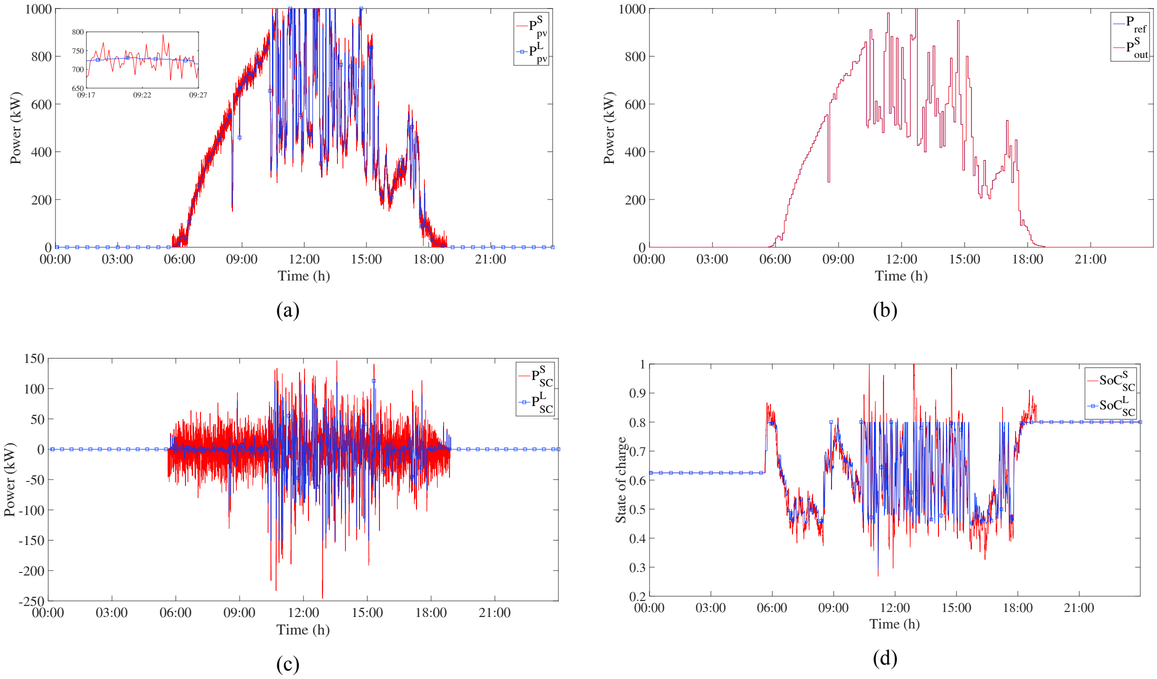

Fig.3. (a) Forecasted PV generation at the upper and bottom layers (b) bottom layer power reference tracking (α=0.5 and β=0.5) (c) Supercapacitor power flows at the upper and bottom layers (d) Supercapacitor SOC at the upper and bottom layers

References

[1] Bocklisch T. Hybrid energy storage systems for renewable energy applications. Energy Procedia. 2015 Jun, 73(2015):103–11.
[2] Abbey C, Strunz K, Joós G. A knowledge-based approach for control of two-level energy storage for wind energy systems. IEEE Trans. Energy Convers. 2009 Jun; 24(2):539–47.
[3] Ding M, Wang B, Chen Z, Chen Z, Luo Y, Zheng G. Stabilizing control strategy of complementary energy storage in renewable energy system. IEEE Innovative Smart Grid Technologies Conference. 21-24 May 2012, Tianjin, China: 1-5.
[4] Wang G, Ciobotaru M, Agelidis VG. Power smoothing of large solar PV plant using hybrid energy storage. IEEE Trans. Sustain. Energy 2014 Jul; 5(3): 834-842.
[5] Choi M, Kim S, Seo S. Energy management optimization in a battery/supercapacitor hybrid energy storage system. IEEE Trans. Smart Grid. 2012 Mar; 3(1): 463-472.
[6] Han X, Chen F, Cui X, Li Y, Li X. A power smoothing control strategy and optimized allocation of battery capacity based on hybrid storage energy technology. Energies. 2012 May; 5(5): 1593-1612
[7] Tazvinga H, Xia X, Zhang J. Minimum cost solution of photovoltaic-diesel-battery hybrid power systems for remote consumers. Solar Energy. 2012 Oct; 96: 292-9.